Saudi Pharmaceutical Journal 28 (2020) 1129–1137

Contents lists available at ScienceDirect

Saudi Pharmaceutical Journal

journal homepage: www.sciencedirect.com

Original article

Phytochemical profile, antioxidant and cytotoxic potential of *Parkinsonia aculeata* L. growing in Saudi Arabia

Sahar Abdelaziz [a], Hanan M. Al Yousef [b,*], Ali S. Al-Qahtani [b], Wafaa H.B. Hassan [a], Omer I. Fantoukh [b,*], May A. El-Sayed [a]

[a] Department of Pharmacognosy, Faculty of Pharmacy, Zagazig University, Zagazig, Egypt
[b] Pharmacognosy Department, College of Pharmacy, King Saud University, Saudi Arabia

ARTICLE INFO

Article history:
Received 11 May 2020
Accepted 2 August 2020
Available online 6 August 2020

Keywords:
Parkinsonia aculeata
Fabaceae
UPLC-ESI-MS/MS
Cytotoxicity
Antioxidant

ABSTRACT

Parkinsonia aculeata L. growing in Saudi Arabia was investigated for its phytochemical profile, antioxidant, and cytotoxic properties. UPLC-ESI-MS/MS was employed as a powerful technique for the characterization of secondary metabolites from a hydroalcoholic extract, dichloromethane, and ethyl acetate fractions of *P. aculeata* L. aerial parts. Sixty-nine compounds (flavonoids, anthocyanins, phenolics and fatty acids) were detected and characterized; flavonoids were the abundant components in the analyzed samples. The dichloromethane fraction was rich in phenolics as vanillic acid hexoside, flavonols as 3,7-dimthylquercetin, and flavones as 3′-hydroxymelanettin. However, the ethyl acetate fraction was rich in flavonoid-*C*-glycosides as luteolin-8-*C*-β-D-glucoside (orientin) and apigenin-8-*C*-glucoside (vitexin), flavonoid- *O*, *C*-diglycosides such as luteolin 7-*O*-[6′′-dihydrogalloyl]-glucosyl-8-*C*-pentosyl-(1 → 2)-glucoside and 2′′-*O*-rhamnosyl isoorientin. These compounds were identified for the first time in dichloromethane and ethyl acetate fractions of Saudi *P. aculeata* L.

Additionally, all the samples were assessed for antioxidant activity using DPPH radical scavenging method and for cytotoxic activity through MTT assay. Accordingly, the most active fraction was the ethyl acetate which showed the highest antioxidant activity (SC_{50} = 57.4 ± 1.2 μg/mL) compared with the positive control, ascorbic acid (SC_{50} = 12.4 ± 0.5 μg/mL) and moderate cytotoxicity against HepG-2 (hepatocellular carcinoma) and MCF-7 (breast carcinoma) cell lines with IC_{50} = 56.9 ± 3.1 and 95.8 ± 3.8 μg/mL, respectively compared with cisplatin (IC_{50} = 3.67 ± 0.22 and 5.71 ± 0.57 μg/mL, respectively for both cell lines). The antioxidant and cytotoxic activities may be attributed to the presence of high percentage of phenolic compounds and hydroxylated flavonoids detected in ethyl acetate fraction using UPLS-ESI-MS/MS.

1. Introduction

Parkinsonia aculeata L. belongs to family Fabaceae, which is the third-largest family of the flowering plants. This family played an essential role in human culture. It contains many useful plants like vegetables, crops, woody, and medicinal plants. *P. aculeata* is a large spiny shrub or a small tree that reaches more than 4 m in height. This plant is grown for its fragrant and elegant yellow flowers (Fadl et al., 2015; Shaiq Ali et al., 2005). Moreover, it has an incredible ability to survive and grow under variable environmental conditions and on different soils (Van Klinken et al., 2009). Survey of the genus *Parkinsonia* revealed the presence of variable classes of compounds such as flavones, flavanones, flavone *C*-glycoside, alkaloids, sterols, tannins, terpenoids, glycerols, carotenoids, saponins, carbohydrates, free amino and fatty acids (Hassan et al., 2019; Sharma et al., 2014).

P. aculeata L. has several reported health merits e.g., antioxidant, hypoglycemic (aqueous fraction of aerial part and bark), hepatoprotective (leaves extract), antispermatogenic (ethanolic extract of stem bark), antimalarial (flowers and leaves), amoebicidal, smooth muscle stimulant, analgesic, anti-inflammatory,

* Corresponding authors at: Office 88, College of Pharmacy, King Saud University, Riyadh, 11451, Saudi Arabia (H.M. Al Yousef). Office 1A5, College of Pharmacy, King Saud University, Riyadh, 11451, Saudi Arabia (O.I. Fantoukh).
E-mail addresses: halyousef@ksu.edu.sa (H.M. Al Yousef), ofantoukh@ksu.edu.sa (O.I. Fantoukh).

Peer review under responsibility of King Saud University.

Production and hosting by Elsevier

https://doi.org/10.1016/j.jsps.2020.08.001
1319-0164/

antipyretic (total alcoholic and aqueous extract of leaves) activities ((Sharma et al., 2014; Gupta et al., 2011; Saha et al., 2011). Orally, the hot aqueous extract of its leaves can be used in pregnant women as an abortifacient agent (Gupta et al., 2011). Reported antimicrobial activity of leaf, stem and flower of *P. aculeata* may be caused by alkaloids, while dried aerial parts and dried stem bark's antimicrobial activity may be attributed to the presence of β-amyrin, palmitic acid, *β*- amyrenone, β- sitosterol, *β*- sitoeryl-*β*-D-glucoside, glycerol *β*-butanoate and daucosterol. However, dried seeds' antimicrobial activity was due to the existence of L-dopa and trytophan amino acid (Gupta et al., 2011). Few kinds of research were carried out on the aerial parts of *P. aculeata* L. growing in Saudi Arabia such as the antimicrobial activity of its essential oil and the chemical composition and biological activities of its aqueous fraction (Al-Youssef and Hassan, 2015; Hassan et al., 2019). Our previous results showed that aqueous fraction of *P. aculeata* L. growing in Saudi Arabia had forty tentatively identified compounds and showed a significant antioxidant activity. However, the chemical composition of the total hydroalcoholic extract, dichloromethane and ethyl acetate fractions were not investigated. Therefore, in the present study, the chemical composition of the total hydroalcoholic extract (PAT), dichloromethane (PAD) and ethyl acetate (PAE) fractions were inspected for the first time by UPLC-ESI-MS/MS to determine their constituents. Sixty-nine flavonoids and phenolic compounds were identified, for the first time in this plant. In addition, the DPPH scavenging and anticancer activities against hepatic (HepG-2) and breast (MCF-7) cell lines were investigated. It seems that the pharmacological activities of natural products have a significant correlation with bioactive compounds contents and the chemical composition in plants. Therefore, the aims of the present study were (i) to explore the phytochemical profile using UPLC coupled with ESI-MS/MS detection, (ii) to find out the antioxidant and anticancer activities of PAD, PAE and PAT; and (iii) to predict the components responsible for antioxidant and anticancer activities.

2. Materials and methods

2.1. Plant materials

The aerial parts of *P. aculeata* L. were collected in 2013 from the Diriyah region, Riyadh city, Saudi Arabia. The plant was verified by Prof Dr. Jakob Thomas; College of Science, KSU and Prof Dr. Husain Abdel Basset, professor of Taxonomy, Faculty of Science, Zagazig University, Egypt. A voucher specimen (#PA-513) was prepared and deposited at the herbarium in the Department of Pharmacognosy, Faculty of Pharmacy, Zagazig University. *P. aculeata* aerial parts were air-dried and ground into coarse particles until use.

2.2. Preparation of extract

Air-dried powdered aerial parts *of P. aculeata* (800 g) were extracted by ethanol (90%, 7 L) at room temperature till complete exhaustion. The extract was evaporated under vacuum to yield 111 g total ethanolic residue (PAT). PAT was suspended in a methanol–water mixture (1:9, 300 ml) and successively partitioned against light petroleum, dichloromethane and ethyl acetate to give 10 g, 4 g and 7 g of light petroleum, dichloromethane (PAD) and ethyl acetate (PAE) fractions respectively.

2.3. UPLC- ESI- MS/MS analysis

Ultra-performance liquid chromatography with electrospray ionization quadrupole-linear ion trap-tandem mass spectrometry analysis, performed on ESI-MS negative ion acquisition mode, was done on a XEVO TQD triple quadruple instrument. The total hydroalcoholic extract (PAT), dichloromethane (PAD) and ethyl acetate (PAE) fractions of *P. aculeata* L. were analyzed by UPLC, in order to acquire chromatographic profiles. HPLC grade methanol was used to dissolve the samples using membrane disc filter (0.2 μm) for filtration, and concentration of the resulting solutions was 100 μg/mL using HPLC grade methanol, then subjected to LC-ESI-MS analysis. The UPLC system was a mass spectrometer, Waters Corporation, Milford, USA. The reverse-phase separations were performed (ACQUITY UPLC BEH C_{18} Column, 1.7 μm–2.1 × 50 mm; 50 mm × 1.2 mm inner diameter; 1.7 μm particle size) at 0.2 m/mL flow rate. A previously reported gradient program was applied for the analysis (Hassan et al., 2019).

The mobile phase consisted of acidified water containing 0.1% formic acid (A) and acidified methanol containing 0.1% formic acid (B). The employed elution conditions were as follows: 0–2 min, isocratic elution at 10% B; 2–5 min, linear gradient from 10 to 30% B; 5–15 min, linear gradient from 30% to 70% B; 15–22 min, linear gradient from 70% to 90% B; and 22–25 min, isocratic elution at 90% B; finally, washing and reconditioning of the column were done. Electrospray ionization (ESI) was performed in negative ion mode to obtain more data. The parameters for analysis were set using negative ion mode as follows: cone voltage 30 eV, source temperature 150 °C, desolvation temperature 440 °C, capillary voltage 3 kV, desolvation gas flow 900 L/h, and cone gas flow 50 L/h. Mass spectra were detected in the ESI between *m*/*z* 100 and 1000 atomic mass units. Chemical constituents were identified by their ESI– QqQLIT–MS/MS spectra and fragmentation patterns. The peaks and spectra were processed using the MassLynx 4.1 software and tentatively identified by comparing their retention time (R_t) and mass spectrum with reported data.

2.4. Antioxidant assay

The antioxidant activity of the total hydroalcoholic extract, dichloromethane, and ethyl acetate fractions of *P. aculeata* L. were determined at the Regional Center for Mycology and Biotechnology (RCMB) at Al- Azhar University using the free radical 2,2-diphyenyl-picrylhydrazyl (DPPH) scavenging assay in triplicate, and average values were considered as described by (Al-Yousef et al., 2020). Freshly prepared (0.1 mM) solution of 2,2-diphenyl-1-picrylhydrazyl (DPPH) and different tested extract/or fractions prepared at 5, 10, 20, 40, 80, 160, and 320 μg/mL in methanol were vigorously mixed and allowed to stand in the dark at room temperature for 30 min. Using UV–visible spectrophotometer (Milton Roy, Spectronic 1201), the absorbance values of the resulting solution were recorded at λ_{max} 517 nm against DPPH radical without antioxidant (control) and the reference compound ascorbic acid (5, 10, 20, 40, 80, 160, and 320 μg/mL). All the determinations were carried out in three replicates and averaged. The percentage inhibition of the DPPH radical was calculated according to the following formula:

$$\%\,\text{DPPH radical} - \text{scavenging} = [\{(\mathbf{AC} - \mathbf{AS})/\mathbf{AC}\} \times \mathbf{100}]$$

where *AC* = Absorbance of the control solution and *AS* = absorbance of the sample in DPPH solution.

Plot the percentage of DPPH radical scavenging against each extract concentration and ascorbic acid (μg/ mL) to determine the concentration required to scavenge DPPH by 50% (i.e., concentration giving 50% reduction in the absorbance of a DPPH solution from its initial absorbance) (SC_{50}).

2.5. Cell culture and cytotoxicity assay

HepG-2 (Human hepatocarcinoma) and MCF-7 (human breast carcinoma) cells were obtained from VACSERA Tissue Culture Unit

and maintained in DMEM supplemented with 10% FBS and 100 μg/ml penicillin–streptomycin-amphotericin B solution. The cytotoxic effects of the total hydroalcoholic extract, dichloromethane, and ethyl acetate fractions of *P. aculeata* L. against HepG-2 and MCF-7 cells were determined using the MTT cell viability assay as described previously (Ramos-Silva et al., 2017)

3. Results and discussion

3.1. Identification of polyphenols and other constituents of P. aculeata fractions by UPLC-ESI-MS/MS

UPLC-ESI-MS/MS, operating in negative ionization mode was used to analyze the crude hydroalcoholic extract (PAT), dichloromethane (PAD) and ethyl acetate fractions (PAE) of *P. aculeata* L. The identification was based on their MS^2 information given by the mass of the precursor ion and their fragments, together with neutral mass loss and known fragmentation patterns for the given classes of compounds as well as comparison with the available literature as shown in Table 1 and Fig. 1**.** Totally, sixty-nine compounds were tentatively identified in the extract and fractions of *P. aculeata*. These compounds comprised phenolic acids and their derivatives, anthocyanins, flavonoids, diterpenes and fatty acids. Table 1 indicates all the identified compounds, their retention times, experimental *m/z* in negative ionization mode, and MS/MS fragments.

3.1.1. Phenolic compounds

The detected phenolic compounds were coumaric acid (**4**) and its isomers (**11, 39**), gallic acid-*O*-malic acid (**26**) (Abu-Reidah et al., 2015), vanillic acid hexoside (**27**) and its isomer (**38**) (Abu-Reidah et al., 2013), *O*-*trans*-feruloyl-malic acid (**41**) (Szajwaj et al., 2011), cinnamoyl-galloylglucose (**50**) (Abu-Reidah et al., 2019) and rosmarinic acid (**60**) (Hossain et al., 2010).

3.1.2. Anthocyanins

Three anthocyanin derivatives have been detected in *P. aculeata* total hydroalcoholic extract and dichloromethane fraction. Compound **12** was tentatively identified as cyanidin as it exhibits a molecular ion at *m/z* 287 (Karar and Kuhnert 2015). 7-*O*-Methyl-cyanidin-3-*O*-galactoside was proposed for compound **20** ($[M-H]^-$ at *m/z* 461), its MS^2 spectral data showed a fragment ion at *m/z* 299 $[M-H-162]^-$, indicating methyl-cyanidin and the neutral loss of galactose moiety (Abu-Reidah et al., 2015).

Compound **65** exhibited molecular ion at *m/z* 613 in the MS spectrum. The product ion in MS/MS spectrum was at *m/z* 299 corresponding to methyl-cyanidin in structure and to the neutral loss of galactose (162 Da) and galloyl (152 Da) moieties. Therefore, the compound was assigned to 7-*O*-methyl-cyanidin-3-*O*-(2′′galloyl)-galactoside (Abu-Reidah et al., 2015).

3.1.3. Flavonoid-C-glycosides

In negative ionization mode, the existence of ($[M-H]^-$-90), and ($[M-H]^-$-120) fragments indicated that these compounds are mono-*C*-hexosylated flavonoids. By investigation of MS^2 spectrum, the absence of the fragment ion at *m/z* ($[M-H]^-$-18) confirmed that the sugar is located on position 8. While the loss of water molecule caused the existence of mass fragment *m/z* ($[M-H]^-$-18), confirmed the presence of *C*-6 glucoside (El-Sayed et al., 2017).

For compounds **1, 6, 14**, and **37**, the ESI-MS spectra showed a deprotonated molecule at *m/z* 447. The MS^2 spectrum on precursor ion exhibited fragments at *m/z* 357 $(M-H-90)^-$ and a base peak at *m/z* 327 $(M-H-120)^-$ which detect the existence of hexose part of *C*-glycoside flavone. Moreover, from the distinguished base peak fragment of compound **1** at *m/z* 327 (aglycone + 41) and short retention time (0.85 min) it could be concluded that compound **1** was identified as kaempferol-8-*C*-*β*-D-glucoside (Hassan et al., 2019) while compounds **6, 14,** and **37** were identified as luteolin-8-*C*-*β*-D-glucopyranoside (orientin) (Hassan et al., 2019).

Diosmetin-8-*C*-glucoside (orientin-4′-methyl ether) (**2**) was characterized by molecular ion at *m/z* 461 ($[M-H]^-$). The MS/MS fragmentation pattern exhibited diagnostic fragment ions at *m/z* 341 $(M-H-120)^-$ which indicated the existence of hexose part of *C*-glycoside flavone (Brito et al., 2014).

For compound **17**, the ESI-MS spectrum gave deprotonated molecule at *m/z* 431, which fragmented further giving fragment ions at *m/z* 341 $(M-H-90)^-$ and a base peak at *m/z* 311 $(M-H-120)^-$, suggesting that the mono-*C*-glycosylation is in position 8. Thus, the absence of the loss of 18 Da, indicate that the sugar substituent is located in position 8. Compound **17** was characterized as vitexin (apigenin-8-*C*-glucoside) (El-Sayed et al., 2017). Vitexin, was previously isolated from *P. aculeata* L. (Hassan et al., 2019)

In the hydroalcoholic extract, one flavone-6,8-di-*C*-glycoside was found. The ESI-MS spectra of compound **9** showed a deprotonated molecule at *m/z* 623 that its consecutive MS^2 fragmentation showed a base peak at *m/z* 383 $(M-H-120-120)^-$ that confirm the two *C*-glucosides substitution. Compound **9** was identified as diosmetin-6,8-di-*C*-glucoside that known as lucenin-2,4′-methyl ether (Brito et al., 2014).

3.1.4. Flavonoid O, C-diglycosides

In the *O, C*-diglycosides flavonoid, the aglycone ion was absent and only the precursor ion $[M-H]^-$ is existed in addition to the interglycosidic linkage cleavage ions including the characteristic fragmentation ions at $[M-H-120]^-$ and $[M-H-120-162]^-$ or $[M-H-120-146]^-$ with or without $[M-H-18]^-$ (Hassan et al., 2019). On the basis of these rules, compound **15** (R_t 8.90 min) with $[M-H]^-$ ion at *m/z* 593 was tentatively identified as 2′′-*O*-rhamnosyl isoorientin as it showed MS^2 fragments at *m/z* 473 $[M-H-120]^-$; corresponding to a loss of *C*-hexose moiety (-120 Da), *m/z* 429 $[M-H-146-18]^-$, corresponding to a loss of *O*-rhamnose moiety (-146 Da) and one water molecule (18 Da) while fragment ion at *m/z* 327 $[M-H-146-120]^-$; corresponding to additional loss of *C*-hexose moiety (-120 Da) as well as the aglycone ion (*m/z* 447) absence is in agreement with an *O, C*-diglycoside structure (Figueirinha et al., 2008).

Compound **64** produced a deprotonated molecular ion at *m/z* 739 and MS^2 ions at *m/z* 431 $[M-H-308]^-$; corresponding to a loss of *O*-neohesperidoside moiety (−308 Da) and *m/z* 311 $[M-H-308-120]^-$; corresponding to additional loss of *C*-hexose moiety (−120 Da) and was identified as apigenin-7-*O*-neohesperidoside-6-*C*-glucoside (Brito et al., 2014).

Compound **13** exhibited a deprotonated molecular ion at *m/z* 895. The MS^2 data showed daughter ions at *m/z* 447, 357 (Ag + 71), and 327 (Ag + 41), corresponding to the loss of a pentosylglucoside with 1 → 2 interglycosidic linkage. The fragment ions observed at *m/z* 357 and 327 are typical of mono-glycosylflavones. The high intensity of the ion at *m/z* 327 (base peak) confirmed the 8-*C* substitution. Therefore compound **13** was assigned as luteolin 7-*O*-[6′′-dihydrogalloyl]-glucosyl-8-*C*-pentosyl-(1 → 2)-glucoside (Benayad et al., 2014).

3.1.5. Flavonoid-O-glucosides, O-galactosides and O-pentoside

The MS^2 fragmentation pattern for compounds **10, 16, 28, 34** and **43** was typical for *O*-glycosyl flavonoids exhibiting fragment at $[M-H-162]^-$ indicating an *O*-glycosilation with a hexose moiety. Compound **10** was identified as chrysoeriol-7-*O*-glucoside as it exhibited a $[M-H]^-$ ion at *m/z* 461 and MS^2 base peak ion at *m/z* 299 $[M-H-162]^-$ after the neutral loss of glucosyl moiety (162 Da) (El-Sayed et al., 2017). Compounds **16** and **34** showed a deprotonated molecular ion at *m/z* 463 with characteristic MS^2

Table 1
Metabolites Identified in *P. aculeata* L. aerial parts hydroalcoholic extract (PAT), dichloromethane (PAD) and ethyl acetate (PAE) fractions using UPLC-ESI-MS/MS analysis in negative ionization mode.

No.	Compound name	R_t (min)	$[M-H]^-$ (*m/z*)	MS^2 fragments (*m/z*)	PAT	PAD	PAE	Ref.
1	Kaempferol-8-*C*-*β*-D-glucopyranoside	0.85	447	357([M−H]$^-$ -90), 327 ([M−H]$^-$ -120), 299, 297 ([M−H]$^-$ -150), 285 ([M−H]$^-$ -162)	+		+	1
2	Diosmetin-8-*C*-glucoside (Orientin-4'-methyl ether)	0.85	461	341	+		+	2
3	Eriodictyol-*O*- glucuronide	0.85	463	287	+		+	3
4	Coumaric acid	5.43	163	119	+	+		4
5	Luteolin-7-*O*-rutinoside	6.47	593	285	+		+	5
6	Luteolin-8-*C*-*β*-D-glucopyranoside(orientin)	7.17	447	357, 327, 299, 297, 285	+		+	1
7	Butin	7.79	271	135	+	+	+	6
8	Eriodictyol	7.92	287	151, 135, 107	+		+	2
9	Diosmetin-6,8-di-*C*-glucoside (Lucenin-2,4'-methyl ether)	8.01	623	383, 312	+			2
10	Chrysoeriol-7-*O*-glucoside	8.10	461	371, 341, 299 ([M−H]$^-$ - 162), 283, 269	+		+	5
11	Coumaric acid isomer	8.23	163	119	+		+	4
12	Cyanidin	8.40	287	151, 135, 107	+	+		7
13	Luteolin-7-*O*-[6''-dihydrogalloyl]-glucosyl-8-*C*-pentosyl-(1→2)-glucoside	8.63	895	447, 357, 339, 327	+		+	8
14	Orientin isomer	8.73	447	357, 327, 299, 297, 285	+		+	1
15	2''-*O*-Rhamnosyl isoorientin	8.90	593	473, 429, 369, 357, 339, 327, 298	+		+	9
16	Quercetin hexoside	9.02	463	301, 179	+		+	10
17	Vitexin	9.37	431	341, 311	+		+	5
18	Butin isomer	9.44	271	135	+		+	6
19	kaempferol-3-*O*-(3'',6''-dicoumaroylglucoside)	9.58	739	285, 284, 254, 227	+			1
20	7-*O*-Methyl-cyanidin-3-*O*-galactoside	9.73	461	299, 298	+			4
21	Diosmetin-7-*O*-rutinoside	9.88	607	299	+			11
22	Quercetin rhamnosyl hexoside	10.04	609	301, 300, 271, 151	+		+	12
23	Butin isomer	10.08	271	135	+		+	6
24	Homoplantaginin	10.53	461	297, 283, 161	+		+	13
25	Acacetin-7-*O*-diglucoside	10.74	607	283	+			1
26	Gallic acid-*O*-malic acid	10.92	285	169, 133	+			4
27	Vanillic acid hexoside	10.97	329	167 [M−H-162]	+	+		14
28	Kaempferol-3-*O*-glucoside	10.99	447	285	+		+	15
29	Kaempferol-3-*O*-rutinoside	11.01	593	285	+		+	5
30	Butin isomer	11.10	271	135	+	+		6
31	Kaempferide derivative	11.19	623	299, 284, 255, 163	+			16
32	Homoplantaginin isomer	11.22	461	297, 283, 161	+		+	13
33	Chrysoeriol	11.24	299	284	+	+		5
34	Quercetin-3-*O*-galactoside	11.25	463	301	+		+	10
35	Kaempferol-3-*O*-rhamnoside	11.55	431	285	+		+	17
36	Carnosol quinone	11.56	327	299	+		+	18
37	Orientin isomer	11.71	447	357, 327, 297	+			1
38	Vanillic acid hexoside isomer	11.97	329	167	+	+		14
39	Coumaric acid isomer	12.11	163	119	+			4
40	Apigenin neohesperidoside	12.22	577	269	+			4
41	*O-trans*-Feruloyl-malic acid	12.32	309	193, 177	+	+		19
42	Homoplantaginin isomer	12.46	461	297, 283, 161	+		+	13
43	Apigenin-7-O-glucoside	12.48	431	269	+			7
44	Luteolin-3'-*O*-rhamnoside	12.50	431	285	+			17
45	3'-hydroxymelanettin	13.52	299	284	+	+		20
46	Kaempferide	13.85	299	284, 255, 163, 107	+		+	16
47	Naringenin methylrhamnoside*	13.90	431	271	+			
48	Lariciresinol	14.00	359	329, 314, 299	+	+		21
49	Methoxycarnosol	14.20	359	329, 285	+	+		22
50	Cinnamoyl-galloylglucose	14.43	461	315, 163, 152	+		+	11
51	Dihydroxypalmitic acid	14.55	287	269	+		+	11
52	Chrysoeriol isomer	15.00	299	284	+		+	5
53	Trihydroxy-octadecadienoic acid	15.03	327	171, 137	+	+		11
54	Trihydroxy-octadecadienoic acid isomer	15.45	327	171, 137	+	+	+	11
55	Carnosol quinone isomer	15.59	327	299	+	+		18
56	3,7-dimethylquercetin	16.04	329	314, 299	+	+		15
57	Dihydroxypalmitic acid isomer	16.23	287	269	+	+		11
58	Trihydroxyoctadeca-10(E)-dienoic acid isomer	16.34	329	229, 211	+	+	+	11
59	Coriolic acid	17.44	295	277, 195, 171	+	+		11
60	Rosmarinic acid	17.70	359	197, 179, 161	+	+		22
61	3,7-dimethylquercetin isomer	18.17	329	314, 299	+	+		15
62	Apigenin-*O*-pentoside	19.99	447	401	+			23
63	3,7-dimethylquercetin isomer	20.29	329	314, 299	+	+		15
64	Apigenin-7-*O*-neohesperidoside-6-*C*-glucoside	20.90	739	431, 311	+			2
65	7-*O*-Methyl-cyanidin-3-*O*-(2''galloyl)-galactoside	21.67	613	299	+	+		4

Table 1 (*continued*)

No.	Compound name	R_t (min)	$[M-H]^-$ (*m/z*)	MS^2 fragments (*m/z*)	PAT	PAD	PAE	Ref.
66	Lanopalmitic acid	24.18	271	225	+	+		11
67	5-Hydroxy-3,4′,7-trimethoxy-flavone	24.50	327	312, 297	+	+		25
68	Lanopalmitic acid isomer	24.99	271	225	+			11
69	Luteolin	28.59	285	269	+	+		11

* = Tentative identified; 1= Hassan et al., 2019; 2= Brito et al., 2014; 3= Ringl et al., 2007; 4= Abu-Reidah et al., 2015; 5= El-Sayed et al., 2017; 6= Jin et al., 2015; 7= Karar & Kuhnert, 2015; 8= Benayad et al., 2014; 9= Figueirinha et al., 2008; 10= Plazonić et al., 2009; 11= Abu-Reidah et al., 2019; 12= Engels et al., 2012; 13= Achour et al., 2018; 14= Abu-Reidah et al., 2013; 15 = Quifer-Rada et al., 2015; 16 = Chernonosov et al., 2017; 17= Li et al., 2014; 18 = Mena et al., 2016; 19= Szajwaj et al., 2011; 20= Liu et al., 2005; 21= Sanz et al., 2012; 22= Hossain et al., 2010; 23 = Spínola et al., 2015; 24= Simirgiotis et al., 2015.

fragment ion at *m/z* 301 $[M-H\text{-glc.}]^-$ which related to deprotonated quercetin and consequently it was tentatively identified as quercetin hexoside and quercetin-3-*O*-galactoside, respectively (Plazonić et al., 2009).

The precursor ion of compound **28** was detected at *m/z* 447 $[M-H]^-$ and its characteristic MS^2 fragment ion at *m/z* 285 $[M-H\text{-}162]^-$ related to deprotonated kaempferol after neutral loss of glucosyl moiety (−162 Da) and consequently it was tentatively identified as kaempferol-3-*O*-glucoside (Quifer-Rada et al., 2015), while compound **43** produced a pseudomolecular ion at *m/z* 431 with main MS^2 fragment at *m/z* 269 $[M-H\text{-}162]^-$ related to deprotonated apigenin and suggesting the neutral loss of glucose moiety (−162 Da) and was tentatively identified as apigenin-7-*O*-glucoside (Karar and Kuhnert 2015).

Homoplantaginin (4′,5,7-trihydroxy-6-methoxyflavone-7-glucoside) (6-methoxyapigenin-7-*O*-glucoside) (**24**) and its isomers (**32** and **42**) were characterized by molecular ion at *m/z* 461 $[M-H]^-$ and diagnostic fragment ions at *m/z* 297 $(M-H\text{-}162\text{-}2H)^-$ related to loss of glucose moiety (−162 Da) and corresponding to methoxyapigenin in structure and *m/z* 283 related to loss of additional methyl moiety (Achour et al., 2018).

The diglucosylated form of acacetin has molecular ion at *m/z* 607 and MS/MS fragment ion at *m/z* 283, which is due to two hexose moieties loss $[M-H\text{-}162\text{-}162]^-$ and corresponding to acacetin in structure. Thus, compound **25** was characterized as acacetin-7-*O*-diglucoside (Hassan et al., 2019).

Kaempferol-3-*O*-(3′′, 6′′-dicoumaroyl glucoside) (**19**) produced a $[M-H]^-$ ion at *m/z* 739 with MS^2 fragments at *m/z* 285 $[M-H\text{-}162\text{-}146\text{-}146]^-$. These were indicative of a kaempoferol with two coumaroyl (2 × 146 Da) and one hexose (162 Da) moieties (Hassan et al., 2019). Apigenin-*O*-pentoside (**62**) was recognized by comparing its MS/MS fragmentation pattern with the reported data (Spínola et al., 2015).

3.1.6. Flavonoid-O-rhamnoside

In the negative ionization mode, compounds **35, 44,** and **47** generated a deprotonated ion at *m/z* 431. In the MS^2 spectrum of compound **35** and **44**, a characteristic ion peak at *m/z* 285 $[M-H\text{-}146]^-$ was observed corresponding to the loss of rhamnosyl moiety. Compounds **35** and **44** were identified as kaempferol-3-*O*-rhamnoside and luteolin-3′-*O*-rhamnoside, respectively (Li et al., 2014). It was difficult to differentiate between the luteolin and kaempferol derivatives by the use of MS^2 data (Abu-Reidah et al., 2019), but the earlier elution of kaempferol before luteolin was distinguished ((Li et al., 2014)

Compound **47** was tentatively identified as naringenin methylrhamnoside. It exhibited a deprotonated molecular ion at *m/z* 431 and intense fragment ion at *m/z* 271 [loss of 160 Da; loss of rhamnose (146 Da) with methyl (14 Da) moieties]. The fragment ion at *m/z* 271 indicated the naringenin aglycone (Li et al., 2014). Methyl rhamnose was previously isolated from the plant kingdom (Ogawa et al., 1997)

3.1.7. Rutinoside and neohesperidoside flavonoids

Rutinosides [Glc (6 → 1) Rha] were eluted before neohesperidosides [Glc(2 → 1)Rha]. The rutinosides favor mostly the complete loss of the disaccharide unit ($[M-H]^-$-308), giving this high abundant specific aglycone peak than that observed for the neohesperidoside (El-Sayed et al., 2017).

Two compounds with deprotonated molecular ion at *m/z* 593 and MS^2 fragment ion at *m/z* 285 ($[M-H]^-$-308) indicated the luteolin/or kaempferol aglycone. Luteolin-7-*O*-rutinoside (**5**), kaempferol-7-*O*-rutinoside (**29**) were identified (El-Sayed et al., 2017).

Other rutinosides were found at R_t 9.88 min (compound **21**) and 10.04 min (compound **22**), the ESI-MS spectrum of compound **21** exhibited a deprotonated molecule at *m/z* 607, which fragmented to give ion peak at *m/z* 299 $(M-H\text{-}308)^-$ which indicated the diosmetin aglycone. Compound **21** was identified as diosmetin-7-*O*-rutinoside (Abu-Reidah et al., 2019). Compound **22** (quercetin rhamnosyl hexoside) exhibited a deprotonated molecule at *m/z* 609, The sequential MS/MS fragmentation of *m/z* 609 allowed the existence of a base peak at *m/z* 301, due to the loss of 308 Da (rhamnose with hexose moieties). Compound **22** might be described as either quercetin with a rhamnogalactoside attached or a rhamnoglucoside with a different correlation from that in rutin (Engels et al., 2012).

Apigenin neohesperidoside (**40**) was identified in the hydroalcoholic extract of *P. aculeata* as it showed a pseudomolecular ion at *m/z* 577 and *m/z* 269 as MS^2 fragment daughter ion after loss of 308 Da corresponding to the neohesperidoside moiety (Abu-Reidah et al., 2015)

3.1.8. Flavonoid -O-glucuronides

Flavonoid-*O*- glucuronide, such as eriodictyol-*O*-glucuronide (**3**), was identified by neutral loss of 176 Da (glucuronide moiety). The precursor ion of compound **3** was detected at *m/z* 463 $[M-H]^-$ and its characteristic MS^2 fragment ion at *m/z* 287 $[M-H\text{-}176]^-$ related to deprotonated eriodictyol (Ringl et al., 2007).

3.1.9. Flavonoid aglycones

Five flavanones were detected in the examined fractions. By comparing MS^2 fragmentation pattern with the previously reported data, eriodictyol (**8**) (Brito et al., 2014) butin (3′,4′,7-trihydroxyflavanone) (5-deoxyeriodictyol) (**7**) and its isomers (**18, 23** and **30**) were identified (Jin et al., 2015).

A total of five flavones (**33, 45, 52, 67** and **69**) have been detected. By comparing MS^2 fragmentation pattern with the reported data, chrysoeriol (**33**) and its positional isomer (**52**)

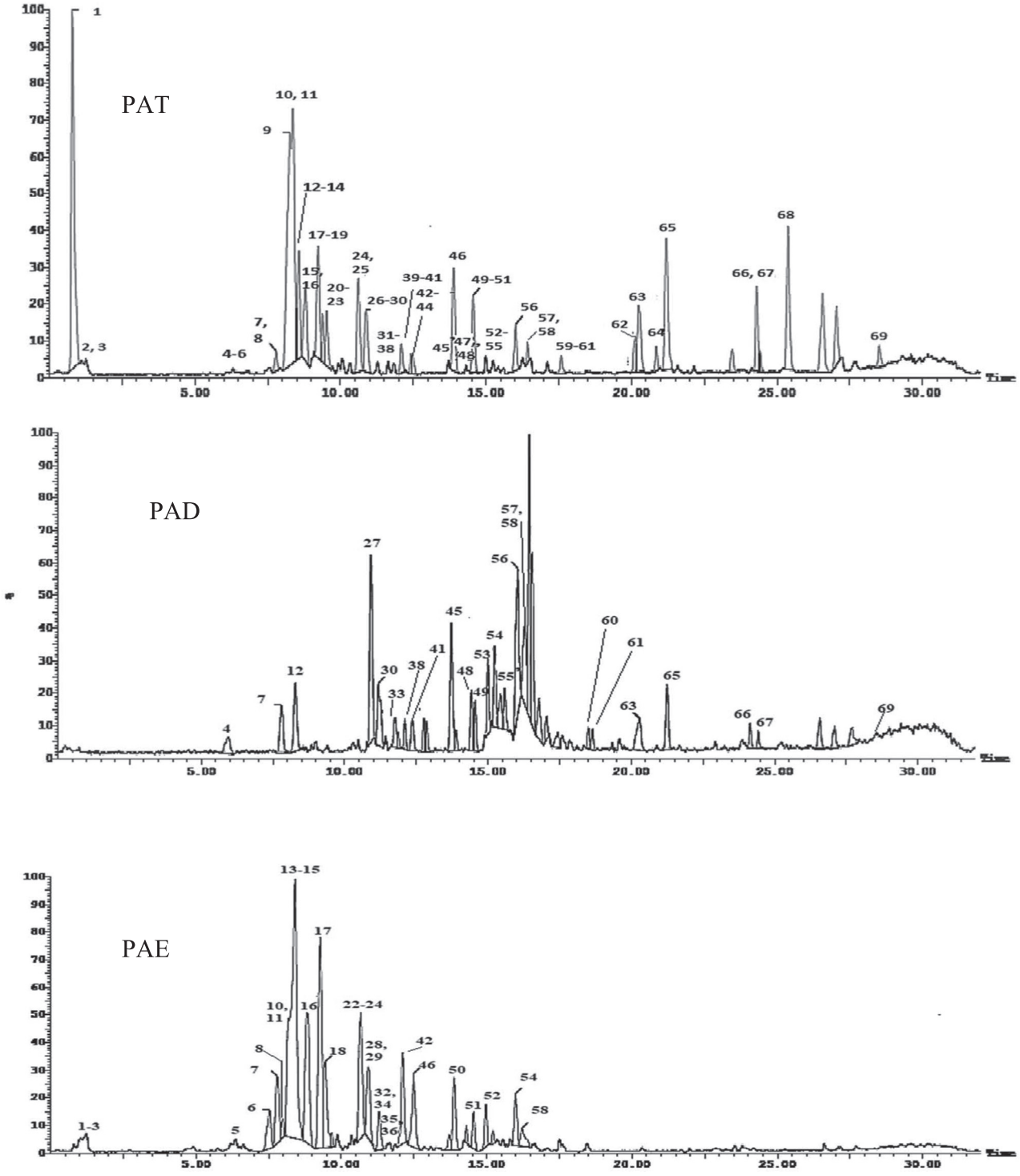

Fig. 1. Chromatograms of *P. aculeata* aerial parts hydroalcoholic extract (PAT), dichloromethane (PAD) and ethyl acetate (PAE) fractions using UPLC-ESI-MS/MS analysis in negative ionization mode.

showed a deprotonated molecular ion at *m*/*z* 299 and an intense fragment at *m*/*z* 284, were recognized (El-Sayed et al., 2017).

One neoflavone (**45**) showed $[M-H]^-$ molecular ion at *m*/*z* 299 and a significant fragment at *m*/*z* 284 $(M-H-CH_3)^-$ that indicate the methoxylated flavonoid. It was tentatively identified as 3′-hydroxymelanettin as previously reported (Liu et al., 2005). Compound **67**, showed a pseudomolecular ion at *m*/*z* 327 producing a daughter fragment at *m*/*z* 312 $(M-H-CH_3)^-$ and *m*/*z* 297 $(M-H-2CH_3)^-$, was identified as 5-hydroxy-3,4′,7-trimethoxyflavone (Simirgiotis et al., 2015), while luteolin (**69**) was identified as previously published (Abu-Reidah et al., 2019).

Five flavonols were detected. Kaempferide (**46**) (kaempferol methyl ether) with $(M-H)^-$ at *m*/*z* 299 and daughter ions at *m*/*z* 284 $(M-H-CH_3)^-$ indicate the methoxylated flavonoid., 255 and 163 and kaempferide derivative (**31**) with $(M-H)^-$ at *m*/*z* 623 and daughter ions at *m*/*z* 299, 284, 255 and 163 were detected (Chernonosov et al., 2017). For 3, 7-dimethylquercetin (**56**) and its two isomers (**61** and **63**), the ESI-MS spectrum exhibited a

deprotonated molecule at *m/z* 329. The MS^2 spectrum on the precursor ion exhibited fragments ions at *m/z* 314 $(M-H-CH_3)^-$ and *m/z* 299 $(M-H-2CH_3)^-$ (Quifer-Rada et al., 2015).

3.1.10. Fatty acids

Eight fatty acids as dihydroxypalmitic acid (**51, 57**), trihydroxyoctadecadienoic acid (**53, 54**), trihydroxyoctadeca-10(E)-dienoic acid (**58**), coriolic acid (**59**) and lanopalmitic acid (**66** and **68**) were identified as previously published (Abu-Reidah et al., 2015).

3.1.11. Miscellaneous compounds

Carnosol quinone (**36** and **55**) showed a deprotonated molecular ion at *m/z* 327 and an intense fragment at *m/z* 299 (Mena et al., 2016). Methoxycarnosol proposed for compound **49** at R_t 14.20 min (*m/z* 359, $[M-H]^-$). In the MS^2 spectrum, the loss of methoxy (−30 Da) moiety gave a fragment ion at *m/z* 329, which corresponds to carnosol in structure in addition to a characteristic fragment ion at *m/z* 285 corresponding to a loss of a carbon dioxide molecule (Hossain et al., 2010). Lariciresinol (**48**) showed a deprotonated molecular ion at *m/z* 359 and daughter ions at *m/z* 329, 314, and 299 (Sanz et al., 2012).

3.2. Biological activity results

3.2.1. Antioxidant activity

Generally, the plant flavonoids and phenols are highly powerful free radical scavengers and antioxidants. Thus, prevention and cure of various diseases mainly linked with free radicals were achieved by using these natural products. Concentrations series ranging from 5 to 320 µg/mL in methanol were used. The DPPH scavenging potential of different fractions of *P. aculeata* L. as well as ascorbic acid and SC_{50} values (the concentration required to scavenge DPPH by 50%) are expressed in Fig. 2 (A & B).

P. aculeata L. ethyl acetate (PAE) fraction showed significant antioxidant activity as indicated by its high DPPH scavenging percentage (77.1%) at 320 µg/mL and low SC_{50} values (57.4 ± 1.2 µg/mL) compared to ascorbic acid with SC_{50} = 14.2 ± 0.5 µg/mL. This activity can be attributed to its contents of vitexin, orientin, and other *C*-glycosides flavonoids as reported earlier (El-Sayed et al., 2017; He et al., 2016; Lam et al., 2016). During this work, apigenin-8-*C*-glucoside (vitexin), luteolin-8-*C*-*β*-D-glucoside (orientin), flavonoid- *O, C*-diglycosides as luteolin 7-*O*-[6″-dihydrogal loyl]-glucosyl-8-*C*-pentosyl-(1 → 2)-glucoside and 2″-*O*-rhamnosyl isoorientin were detected in LC-MS analysis of ethyl acetate fraction as the most abundant compounds.

Unfortunately, both PAD and PAT fractions showed moderate antioxidant activity than the PAE with SC_{50} = 143.2 ± 0.8 & 133.5 ± 1.3 µg/mL respectively, these results supported the previous literature about the antioxidant potential of *P. aculeata* L. and confirmed its ethnomedical use in the treatment of jaundice (Mruthunjaya and Hukkeri 2008).

Phenolic compounds exhibited many possible mechanisms to act as antioxidants such as free radical scavenging, inhibiting free radical formation, oxygen radical absorbance, peroxide decomposition, increasing the levels of endogenous defenses, chelating of metal ions, suppression of singlet oxygen, and enzymatic inhibition

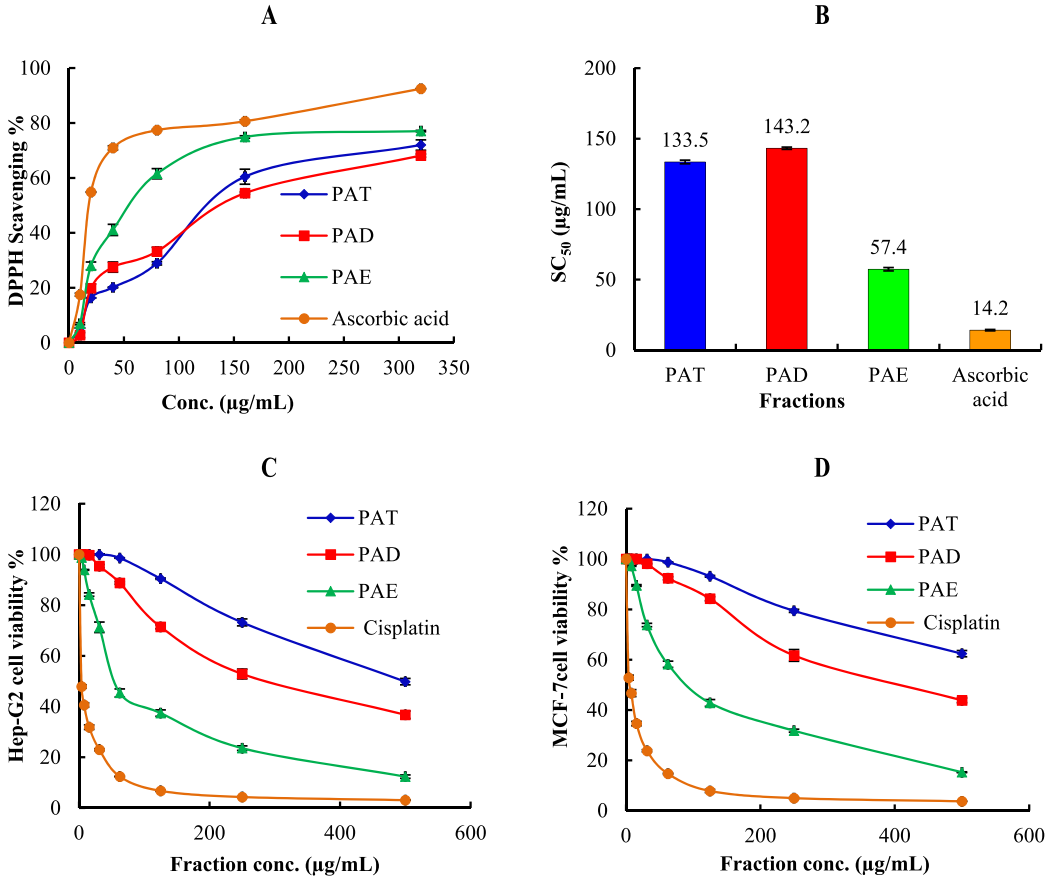

Fig. 2. (A): 2, 2-diphyenyl-picrylhydrazyl (DPPH) radical scavenging activity of different concentrations (5–320 µg/ml) of *P. aculeata* extract and its fractions data are presented as averages ± standard deviations from three experiments. **(B):** SC_{50} of antioxidant activity of *P. aculata* extract, its fractions and ascorbic acid. **(C):** Cytotoxic activity of *P. aculata* extract and its fractions against HepG-2 cell line at different concentrations **(D):** Cytotoxic activity of *P. aculata* extract and its fractions against MCF-7 cell line at different concentrations. **PAT,** total hydroalcoholic extract; **PAD,** dichloromethane fraction and **PAE** ethyl acetate fraction.

Table 2
IC_{50} of the hydroalcoholic extract (PAT), dichloromethane (PAD), ethyl acetate (PAE) fractions of the aerial parts of *P. aculeata* L against HepG-2 and MCF-7carcinoma cell lines.

Tested fraction				
Cell line	IC_{50} (μg/mL)			
	PAT	PAD	PAE	Cisplatin
HepG-2 (Hepatocellular carcinoma)	498 ± 23.4	294 ± 11.3	56.9 ± 3.1	3.67 ± 0.22
MCF-7 (Breast carcinoma)	>500	414 ± 13.6	95.8 ± 3.8	5.71 ± 0.57

These are the mean of three determinations.

(Al-Yousef et al., 2020). The total polyphenolic content is directly related to the antioxidant activity as polyphenolic compounds on a large proportion may be responsible for the antioxidant activity (Obouayeba et al., 2014). Considerable correlation between SC_{50} values, radical scavenging ability, and the identified phenolics and/or flavonoids in LC-MS analysis is proofed as extracts with higher flavonoids and/or phenolics contents displayed lower SC_{50} value and higher antioxidant activity (Al-Yousef et al., 2020).

3.2.2. Cytotoxic activity

Cancer in low- and middle-income countries caused about 70% of death (Kuete et al., 2017). About 15–25% of all females cancer cases and deaths were caused by breast cancer while universally the second major cause of cancer death in males was liver cancer (Torre et al., 2015). In recent times, plant-derived compounds and natural products are promising cancer therapy (Al-Abbasi et al., 2016; Solowey et al., 2014; Wannes et al., 2017) It is necessary for new efficient anticancer drug discovery to check the cytotoxicity of the plant extracts and natural products (Omosa et al., 2016).

In vitro Cytotoxic activity of PAD & PAE fractions and PAT were investigated against HepG-2 and MCF-7 cell lines using MTT assay and cisplatin as a positive standard showed a diminution in cell viability in dose-dependent manner as shown in Fig. 2 (C &D) and Table 2. Estimation was based on IC_{50} values as follows: IC_{50} - $\leq$ 20 μg/mL, highly active; IC_{50} = 21–200 μg/mL, moderately active; $IC5_0$ = 201–500 μg/mL, weakly active; and IC_{50} > 501 μg/mL, inactive, which is in a good accordance with the American National Cancer Institute protocol (Al-Yousef et al., 2020)The results showed that PAE possesses a moderate cytotoxic activity with IC_{50} = 56.9 ± 3.1 and 95.8 ± 3.8 μg/mL for HepG-2 and MCF-7cell lines compared to cisplatin with IC_{50} = 3.67 ± 0.22 and 5.71 ± 0.57 μg/ml, respectively. PAE activity may be attributed to the presence of vitexin (He et al., 2016), homoplantaginin (Genc et al., 2020), orientin (Lam et al., 2016) and butin (3′,4′,7-trihydroxyflavanone) (Zhang et al., 2011). During this work, vitexin, orientin, homoplantaginin, and butin were detected in LC-MS analysis of ethyl acetate fraction as major compounds. However, The PAT exhibited weak cytotoxic activity against HepG-2 and inactive against MCF-7 cell line. The PAD fraction showed weak cytotoxic activity against both cell lines with IC_{50} of 294 ± 11.3 and 414 ± 13.6 μg/mL respectively, when compared to cisplatin 3.67 ± 0.22 and 5.71 ± 0.57 μg/mL (Fig. 2 C & D and Table 2).

4. Conclusion

In conclusion, our results revealed that phenolic compounds, flavonoids, and anthocyanins were identified in hydroalcoholic extract, dichloromethane, and ethyl acetate fractions of *P. aculeata* L. aerial parts using UPLC-ESI-MS/MS analysis. The ethyl acetate fraction of *P. aculeata* L. showed significant *in vitro* antioxidant and cytotoxic activities compared to the other tested fractions (total hydroalcoholic extract and the dichloromethane fraction). These activities might be attributed to its contents of phenolic compounds (such as coumaric acid and cinnamoyl-galloylglucose) and polyhydroxylated flavonoids (such as chrysoeriol-7-*O*-glucoside; luteolin-7-*O*-[6′′-dihydrogalloyl]-glucosyl-8-*C*-pentosyl-(1 → 2)-glucoside; 2′′-*O*-rhamnosyl isoorientin; orientin; vitexin; quercetin hexoside; quercetin rhamnosyl hexoside; butin and homoplantaginin) detected in this fraction. Further studies are planned to isolate and identify the major bioactive compounds from this fraction using various spectroscopic techniques for future *in vivo* investigation.

PAD showed weak cytotoxic activity against both cell lines with IC_{50} of 294 ± 11.3 and 414 ± 13.6 μg/mL, respectively that may be attributed to the presence of anthocyanins as cyanidin and 7-*O*-methyl-cyanidin-3-*O*-(2′′galloyl)- galactoside. Unfortunately, the PAT exhibited weak cytotoxic activity against HepG-2 and inactive against MCF-7 cell line.

Declaration of Competing Interest

The authors declare that they have no known competing financial interests or personal relationships that could have appeared to influence the work reported in this paper.

Acknowledgement

Authors are thankful to the Researchers supporting project number (RSP-2020/132), King Saud University, Riyadh, Saudi Arabia.

The authors thank **Prof Dr. Jakob Thomas,** College of Science, King Saud University, Riyadh, Kingdom of Saudi Arabia (KSU) and **Prof Dr. Husain Abdel Basset,** professor of Taxonomy, Faculty of Science, Zagazig University, Egypt for the plant identification.

Authors' contributions

All authors made considerable contributions to the manuscript. HA, AA, ME, WH, OF and SA designed the study. WH, HA, SA, ME and OF performed the experiments. MA, AA, SA,WH and HA interpreted the results. ME, SA and HA wrote the manuscript. All authors revised the manuscript and confirmed it for publication.

References

Abu-Reidah, I.M., Ali-Shtayeh, M.S., Jamous, R.M., Arráez-Román, D., Segura-Carretero, A., 2015. HPLC–DAD–ESI-MS/MS screening of bioactive components from *Rhus coriaria* L. (Sumac) fruits. Food Chem. 166, 179–191.

Abu-Reidah, I.M., Arráez-Román, D., Al-Nuri, M., Warad, I., Segura-Carretero, A., 2019. Untargeted metabolite profiling and phytochemical analysis of *Micromeria fruticosa* L. (Lamiaceae) leaves. Food Chem. 279, 128–143.

Abu-Reidah, I.M., Arráez-Román, D., Segura-Carretero, A., Fernández-Gutiérrez, A., 2013. Profiling of phenolic and other polar constituents from hydro-methanolic extract of watermelon (*Citrullus lanatus*) by means of accurate-mass spectrometry (HPLC–ESI–QTOF–MS). Food Res. Int. 51 (1), 354–362.

Achour, M., Saguem, S., Sarriá, B., Bravo, L., Mateos, R., 2018. Bioavailability and metabolism of rosemary infusion polyphenols using Caco-2 and HepG2 cell model systems. J. Sci. Food Agric. 98 (10), 3741–3751.

Al-Abbasi, F.A., Alghamdi, E.A., Baghdadi, M.A., Alamoudi, A.J., El-Halawany, A.M., El-Bassossy, H.M., Aseeri, A.H., Al-Abd, A.M., 2016. Gingerol synergizes the cytotoxic effects of doxorubicin against liver cancer cells and protects from its vascular toxicity. Molecules 21 (7), 886.

Al-Yousef, H.M., Hassan, W.H., Abdelaziz, S., Amina, M., Adel, R., El-Sayed, M.A., 2020. UPLC-ESI-MS/MS profile and antioxidant, cytotoxic, antidiabetic, and antiobesity activities of the aqueous extracts of three different *Hibiscus* Species. J. Chem. 2020.

Al-Youssef, H., Hassan, W., 2015. Antimicrobial and antioxidant activities of *Parkinsonia aculeata* and chemical composition of their essential oils. Merit Res. J. Med. Med. Sci. 3, 147–157.

Benayad, Z., Gómez-Cordovés, C., Es-Safi, N., 2014. Characterization of flavonoid glycosides from fenugreek (*Trigonella foenum-graecum*) crude seeds by HPLC–DAD–ESI/MS analysis. Int. J. Mol. Sci. 15 (11), 20668–20685.

Brito, A., Ramirez, J., Areche, C., Sepúlveda, B., Simirgiotis, M., 2014. HPLC-UV-MS profiles of phenolic compounds and antioxidant activity of fruits from three citrus species consumed in Northern Chile. Molecules 19 (11), 17400–17421.

Chernonosov, A.A., Karpova, E.A., Lyakh, E.M., 2017. Identification of phenolic compounds in *Myricaria bracteata* leaves by high-performance liquid chromatography with a diode array detector and liquid chromatography with tandem mass spectrometry. Revista Brasileira de Farmacognosia 27 (5), 576–579.

El-Sayed, M.A., Al-Gendy, A.A., Hamdan, D.I., El-Shazly, A.M., 2017. Phytoconstituents, LC-ESI-MS profile, antioxidant and antimicrobial activities of *Citrus x limon* L. Burm. f. cultivar variegated pink lemon. J. Pharm. Sci. Res. 9 (4), 375–391.

Engels, C., Gräter, D., Esquivel, P., Jiménez, V.M., Gänzle, M.G., Schieber, A., 2012. Characterization of phenolic compounds in jocote (*Spondias purpurea* L.) peels by ultra high-performance liquid chromatography/electrospray ionization mass spectrometry. Food Res. Int. 46 (2):557–562.

Fadl, M.A., Farrag, H.F., Al-Sherif, E., 2015. Floristic composition and vegetation analysis of wild legumes in Taif district, Saudi Arabia. Int. Res. J. Agric. Sci. Soil Sci. 5 (2), 74–80.

Figueirinha, A., Paranhos, A., Pérez-Alonso, J.J., Santos-Buelga, C., Batista, M.T., 2008. *Cymbopogon citratus* leaves: Characterization of flavonoids by HPLC–PDA–ESI/MS/MS and an approach to their potential as a source of bioactive polyphenols. Food Chem. 110 (3), 718–728.

Genc, Y., Dereli, F.T.G., Saracoglu, I., Akkol, E.K., 2020. The inhibitory effects of isolated constituents from *Plantago* major subsp. major L. on collagenase, elastase and hyaluronidase enzymes: potential wound healer. Saudi Pharm. J. 28 (1), 101–106.

Gupta, M.K., Kenganora, M., Banerjee, A., Saini, L., Kumar, V., 2011. Pharmacognostical and phytochemical evaluation on the bark of *Parkinsonia aculeata* Linn. J. Pharm. Sci. Biosci. Res. 1, 86–92.

Hassan, W.H., Abdelaziz, S., Al Yousef, H.M., 2019. Chemical composition and biological activities of the aqueous fraction of *Parkinsonea aculeata* L. growing in Saudi Arabia. Arabian J. Chem. 12 (3):377–387.

He, M., Min, J.-W., Kong, W.-L., He, X.-H., Li, J.-X., Peng, B.-W., 2016. A review on the pharmacological effects of vitexin and isovitexin. Fitoterapia 115, 74–85.

Hossain, M.B., Rai, D.K., Brunton, N.P., Martin-Diana, A.B., Barry-Ryan, C., 2010. Characterization of phenolic composition in Lamiaceae spices by LC-ESI-MS/MS. J. Agric. Food. Chem. 58 (19), 10576–10581.

Jin, M.J., Kim, I.S., Rehman, S.U., Dong, M.-S., Na, C.-S., Yoo, H.H., 2015. A liquid chromatography–tandem mass spectrometry method for simultaneous quantitation of 10 bioactive components in *rhus verniciflua* extracts. J. Chromatogr. Sci. 54 (3), 390–396.

Karar, M.E., Kuhnert, N., 2015. UPLC-ESI-Q-TOF-MS/MS characterization of phenolics from *Crataegus monogyna* and *Crataegus laevigata* (Hawthorn) leaves, fruits and their herbal derived drops (Crataegutt Tropfen). J. Chem. Biol. Therap. 1, 1–23.

Kuete, V., Fokou, F.W., Karaosmanoğlu, O., Beng, V.P., Sivas, H., 2017. Cytotoxicity of the methanol extracts of *Elephantopus mollis*, *Kalanchoe crenata* and 4 other Cameroonian medicinal plants towards human carcinoma cells. BMC Complement. Alternat. Med. 17 (1), 280.

Lam, K.Y., Ling, A.P.K., Koh, R.Y., Wong, Y.P., Say, Y.H., 2016. A review on medicinal properties of orientin. Adv. Pharmacol. Sci. 2016.

Li, R., Liu, S.-k., Song, W., Wang, Y., Li, Y.-j., Qiao, X., Liang, H., Ye, M., 2014. Chemical analysis of the Tibetan herbal medicine *Carduus acanthoides* by UPLC/DAD/qTOF-MS and simultaneous determination of nine major compounds. Anal. Methods 6 (18), 7181–7189.

Liu, R., Ye, M., Guo, H., Bi, K., Da, G., 2005. Liquid chromatography/electrospray ionization mass spectrometry for the characterization of twenty-three flavonoids in the extract of *Dalbergia odorifera*. Rapid Commun. Mass Spectromet.: Int. J. Devoted Rapid Dissemination Up-to-the-Minute Research in Mass Spectrometry 19 (11), 1557–1565.

Mena, P., Cirlini, M., Tassotti, M., Herrlinger, K., Dall'Asta, C., Del Rio, D., 2016. Phytochemical profiling of flavonoids, phenolic acids, terpenoids, and volatile fraction of a rosemary (*Rosmarinus officinalis* L.) extract. Molecules 21 (11), 1576.

Mruthunjaya, K., Hukkeri, V., 2008. *In vitro* antioxidant and free radical scavenging potential of *Parkinsonia aculeata* Linn. Pharmacognosy Magazine 4 (13), 42.

Obouayeba, A., Djyh, N., Diabate, S., Djaman, A., N'guessan, J., Kone, M., Kouakou, T., 2014. Phytochemical and antioxidant activity of Roselle (*Hibiscus sabdariffa* L.) petal extracts. Res. J. Pharm. Biol. Chem. Sci. 5 (2), 1453–1465.

Ogawa, K., Yamaura, M., Maruyama, I., 1997. Isolation and identification of 2-*O*-methyl-L-rhamnose and 3-*O*-methyl-L-rhamnose as constituents of an acidic polysaccharide of *Chlorella vulgaris*. Biosci. Biotechnol. Biochem. 61 (3), 539–540.

Omosa, L.K., Midiwo, J.O., Masila, V.M., Gisacho, B.M., Munayi, R., Chemutai, K.P., Elhaboob, G., Saeed, M.E., Hamdoun, S., Kuete, V., 2016. Cytotoxicity of 91 Kenyan indigenous medicinal plants towards human CCRF-CEM leukemia cells. J. Ethnopharmacol. 179, 177–196.

Plazonić, A., Bucar, F., Maleš, Ž., Mornar, A., Nigović, B., Kujundžić, N., 2009. Identification and quantification of flavonoids and phenolic acids in burr parsley (*Caucalis platycarpos* L.), using high-performance liquid chromatography with diode array detection and electrospray ionization mass spectrometry. Molecules 14 (7), 2466–2490.

Quifer-Rada, P., Vallverdú-Queralt, A., Martínez-Huélamo, M., Chiva-Blanch, G., Jáuregui, O., Estruch, R., Lamuela-Raventós, R., 2015. A comprehensive characterisation of beer polyphenols by high resolution mass spectrometry (LC–ESI-LTQ-Orbitrap-MS). Food Chem. 169, 336–343.

Ramos-Silva, A., Tavares-Carreon, F., Figueroa, M., De la Torre-Zavala, S., Gastelum-Arellanez, A., Rodriguez-Garcia, A., Galan-Wong, L.J., Aviles-Arnaut, H., 2017. Anticancer potential of *Thevetia peruviana* fruit methanolic extract. BMC Complement. Alternat. Med. 17 (1), 241. https://doi.org/10.1186/s12906-017-1727-y.

Ringl, A., Prinz, S., Huefner, A., Kurzmann, M., Kopp, B., 2007. Chemosystematic value of flavonoids from *Crataegus x macrocarpa* (Rosaceae) with special emphasis on (*R*)- and (*S*)-eriodictyol-7-*O*-glucuronide and luteolin-7-*O*-glucuronide. Chem. Biodivers. 4 (2), 154–162. https://doi.org/10.1002/cbdv.200790020.

Saha, D., Mandal, S., Biswal, B., Dash, A.K., Mishra, J., Lanjhiyana, S., 2011. Anti diabetic activity of the bark of *Parkinsonia aculeata* in streptozotocin induced diabetic rats. Int. J. Appl. Biol. Pharm. Technol. (PIJABPT).

Sanz, M., de Simón, B.F., Cadahía, E., Esteruelas, E., Muñoz, A.M., Hernández, T., Estrella, I., Pinto, E., 2012. LC-DAD/ESI-MS/MS study of phenolic compounds in ash (*Fraxinus excelsior* L. and *F. americana* L.) heartwood. Effect of toasting intensity at cooperage. J. Mass Spectrom. 47 (7):905–918.

Shaiq Ali, M., Ahmed, F., Kashif Pervez, M., Azhar, I., Ibrahim, S.A., 2005. Parkintin: A new flavanone with epoxy-isopentyl moiety from *Parkinsonia aculeata* linn. (Caesalpiniaceae). Nat. Prod. Res. 19 (1):53–56.

Sharma, K., Sharma, A., Sharma, M., Tanwar, K., 2014. Isolation of orientin and vitexin from stem bark of *Parkinsonia aculeata* (Caesalpiniaceae) and their successive blending on sheep wool fiber. Int. J. Pharmacogn. Phytochem. Res. 6 (3), 557–561.

Simirgiotis, M., Benites, J., Areche, C., Sepúlveda, B., 2015. Antioxidant capacities and analysis of phenolic compounds in three endemic Nolana species by HPLC-PDA-ESI-MS. Molecules 20 (6), 11490–11507.

Solowey, E., Lichtenstein, M., Sallon, S., Paavilainen, H., Solowey, E., Lorberboum-Galski, H., 2014. Evaluating medicinal plants for anticancer activity. Sci. World J. 2014.

Spínola, V., Pinto, J., Castilho, P.C., 2015. Identification and quantification of phenolic compounds of selected fruits from Madeira Island by HPLC-DAD–ESI-MSn and screening for their antioxidant activity. Food Chem. 173, 14–30.

Szajwaj, B., Moldoch, J., Masullo, M., Piacente, S., Oleszek, W., Stochmal, A., 2011. Amides and esters of phenylpropenoic acids from the aerial parts of *Trifolium pallidum*. Nat. Prod. Commun. 6 (9). 1934578X1100600921.

Torre, L.A., Bray, F., Siegel, R.L., Ferlay, J., Lortet-Tieulent, J., Jemal, A., 2015. Global cancer statistics, 2012. CA Cancer J Clin. 65 (2), 87–108.

Van Klinken, R.D., Campbell, S.D., Heard, T.A., McKenzie, J., March, N., 2009. The Biology of Australian weeds: 54'.*Parkinsonia aculeata*'L. Plant Prot. Q. 24 (3), 100.

Wannes, W.A., Tounsi, M.S., Marzouk, B., 2017. A review of Tunisian medicinal plants with anticancer activity. J. Complement. Integr. Med. 15 (1).

Zhang, R., Lee, I.K., Piao, M.J., Kim, K.C., Kim, A.D., Kim, H.S., Chae, S., Kim, H.S., Hyun, J.W., 2011. Butin (7, 3′, 4′-trihydroxydihydroflavone) reduces oxidative stress-induced cell death via inhibition of the mitochondria-dependent apoptotic pathway. Int. J. Mol. Sci. 12 (6), 3871–3887.